Title
Search for Low-energy Electron Antineutrinos in KamLAND Associated with Gravitational Wave Events

Journal
Astrophysical Journal, 909(2)

ISSN
0004-637X

Authors
Abe, S
Asami, S
Gando, A
et al.

Publication Date
2021-03-10

DOI
10.3847/1538-4357/abd5bc

Peer reviewed

Draft version December 23, 2020
Typeset using LaTeX **preprint** style in AASTeX63

Search for Low-energy Electron Antineutrinos in KamLAND Associated with Gravitational Wave Events

S. Abe,[1] S. Asami,[1] A. Gando,[1] Y. Gando,[1] T. Gima,[1] A. Goto,[1] T. Hachiya,[1] K. Hata,[1] S. Hayashida,[1,2] K. Hosokawa,[1] K. Ichimura,[1] S. Ieki,[1] H. Ikeda,[1] K. Inoue,[1,3] K. Ishidoshiro,[1] Y. Kamei,[1] N. Kawada,[1] Y. Kishimoto,[1,3] T. Kinoshita,[1] M. Koga,[1,3] N. Maemura,[1] T. Mitsui,[1] H. Miyake,[1] K. Nakamura,[1] K. Nakamura,[1] R. Nakamura,[1] H. Ozaki,[1,4] T. Sakai,[1] H. Sambonsugi,[1] I. Shimizu,[1] J. Shirai,[1] K. Shiraishi,[1] A. Suzuki,[1] Y. Suzuki,[1] A. Takeuchi,[1] K. Tamae,[1] K. Ueshima,[1,5] Y. Wada,[1] H. Watanabe,[1] Y. Yoshida,[1] S. Obara,[6] A. Kozlov,[3,7] D. Chernyak,[3,8] Y. Takemoto,[9,10] S. Yoshida,[9] S. Umehara,[11] K. Fushimi,[12] A.K. Ichikawa,[13] K.Z. Nakamura,[13] M. Yoshida,[13] B. E. Berger,[14,3] B.K. Fujikawa,[14,3] J.G. Learned,[15] J. Maricic,[15] S. Axani,[16] L. A. Winslow,[16] Z. Fu,[16] J. Ouellet,[16] Y. Efremenko,[17,3] H. J. Karwowski,[18,19] D. M. Markoff,[18,20] W. Tornow,[18,21,3] A. Li,[19] J. A. Detwiler,[22,3] S. Enomoto,[22,3] M.P. Decowski,[23,3] C. Grant,[24] T. O'Donnell,[25] S. Dell'Oro,[25]

(KamLAND Collaboration)

[1] *Research Center for Neutrino Science, Tohoku University, Sendai 980-8578, Japan*
[2] *Present address: Imperial College London, Department of Physics, Blackett Laboratory, London SW7 2AZ, UK*
[3] *Institute for the Physics and Mathematics of the Universe, The University of Tokyo, Kashiwa 277-8568, Japan*
[4] *Graduate Program on Physics for the Universe, Tohoku University, Sendai 980-8578, Japan*
[5] *Present address: National Institutes for Quantum and Radiological Science and Technology (QST), Hyogo 679-5148, Japan*
[6] *Frontier Research Institute for Interdisciplinary Sciences, Tohoku University, Sendai, 980-8578, Japan*
[7] *Present address: National Research Nuclear University "MEPhI" (Moscow Engineering Physics Institute), Moscow, 115409, Russia*
[8] *Present address: Department of Physics and Astronomy, University of Alabama, Tuscaloosa, Alabama 35487, USA and Institute for Nuclear Research of NASU, 03028 Kyiv, Ukraine*
[9] *Graduate School of Science, Osaka University, Toyonaka, Osaka 560-0043, Japan*
[10] *Present address: Kamioka Observatory, Institute for Cosmic-Ray Research, The University of Tokyo, Hida, Gifu 506-1205, Japan*
[11] *Research Center for Nuclear Physics (RCNP), Osaka University, Ibaraki, Osaka 567-0047, Japan*
[12] *Graduate School of Advanced Technology and Science, Tokushima University, Tokushima, 770-8506, Japan*
[13] *Department of Physics, Kyoto University, Kyoto 606-8502, Japan*
[14] *Nuclear Science Division, Lawrence Berkeley National Laboratory, Berkeley, CA 94720, USA*
[15] *Department of Physics and Astronomy, University of Hawaii at Manoa, Honolulu, Hawaii 96822, USA*
[16] *Massachusetts Institute of Technology, Cambridge, Massachusetts 02139, USA*
[17] *Department of Physics and Astronomy, University of Tennessee, Knoxville, Tennessee 37996, USA*
[18] *Triangle Universities Nuclear Laboratory, Durham, North Carolina 27708, USA and Physics Departments at Duke University, North Carolina Central University, and the University of North Carolina at Chapel Hill*
[19] *The University of North Carolina at Chapel Hill, Chapel Hill, North Carolina 27599, USA*

Corresponding author: S. Obara
shuhei.obara.d4@tohoku.ac.jp

[20]North Carolina Central University, Durham, North Carolina 27701, USA
[21]Physics Department at Duke University, Durham, North Carolina 27705, USA
[22]Center for Experimental Nuclear Physics and Astrophysics, University of Washington, Seattle, Washington 98195, USA
[23]Nikhef, Science Park 105, 1098 XG Amsterdam, The Netherlands
[24]Boston University, Boston, Massachusetts 02215, USA
[25]Center for Neutrino Physics, Virginia Polytechnic Institute and State University, Blacksburg, Virginia 24061, USA

Submitted to ApJ

ABSTRACT

We present the results of a search for MeV-scale electron antineutrino events in KamLAND in coincident with the 60 gravitational wave events/candidates reported by the LIGO/Virgo collaboration during their second and third observing runs. We find no significant coincident signals within a $\pm 500\,\mathrm{s}$ timing window from each gravitational wave and present 90% C.L. upper limits on the electron antineutrino fluence between 10^8–$10^{13}\,\mathrm{cm}^2$ for neutrino energies in the energy range of 1.8–111 MeV.

Keywords: neutrinos — gravitational waves

1. INTRODUCTION

In 2015, gravitational waves (GWs) were first detected by the Advanced Laser Interferometer Gravitational-wave Observatory (LIGO) (Abbott et al. 2016). This event was shown to have originated from the merger of a binary black hole (BBH) system. Nearly two years earlier, the IceCube collaboration published the first observational evidence for high-energy astrophysical neutrinos (Aartsen et al. 2013). The gravitational and weak forces along with the electromagnetic were added to the astronomical observations, beginning a new era of extra-galactic multi-messenger astronomy.

In 2017, LIGO detected an event consistent with a comparably nearby binary neutron-star (BNS) merger (Abbott et al. 2017a). Within seconds of the GW, the electromagnetic counterpart was observed by the *Fermi* Gamma Ray Burst Monitor (Abbott et al. 2017b), making this the first GW multi-messenger event. The online neutrino telescopes – including IceCube, ANTARES, and the Pierre Auger Observatory – did not detect any directionally coincident high-energy (GeV–EeV) neutrinos or an MeV neutrino burst signal (Albert et al. 2017a). While no coincident neutrinos were found, this is consistent with model predictions for the merger (Kimura et al. 2017). In contrast with BBH mergers, BNS mergers are expected to emit neutrinos at both GeV and MeV energies (Mészáros 2017). MeV-scale neutrinos would be produced by the hot collapsing fireball at the beginning of a gamma-ray burst (Sahu & D'Olivo 2005), so we can be confident that they must be produced when there is collapsing matter outside of a black hole. These neutrinos are modeled in several ways, but have energies on the order of the dominant photon energy, and are considerably more numerous than the emitted photons (Halzen & Jaczko 1996). In the case of a post-merger neutron star remnant, thermal emission of MeV neutrinos is expected as the remnant cools (Foucart et al. 2016). The neutron rich environment also suggests a brighter $\bar{\nu}_e$ flux than the ν_e flux (Kyutoku & Kashiyama 2018).

Recently, the LIGO/Virgo collaboration published their event catalog (Abbott et al. 2019), including the full dataset from their first and second observing runs, LIGO-O1 and LIGO-O2 respectively. During the third observing run, LIGO-O3, the LIGO/Virgo collaboration initiated the online GW candidate event database (GraceDB) (LIGO Scientific Collaboration 2020), providing public alerts and a centralized location for aggregating and retrieving event information. For such transient GW events, various neutrino detectors reported correlation searches: Super-Kamiokande (Abe et al. 2016, 2018), Borexino (Agostini et al. 2017), NOvA (Acero et al. 2020), Bikal-GVD Neutrino Telescope (Avrorin et al. 2018), Daya Bay (An et al. 2020), XMASS (Collaboration et al. 2020), and IceCube/ANTARES (Adrián-Martínez et al. 2016; Albert et al. 2017b; Aartsen et al. 2020). The Kamioka Liquid scintillator AntiNeutrino Detector (KamLAND) has also performed a search for electron antineutrinos in coincident with gravitational waves GW150914 and GW151226, and then candidate event LVT151012 (Gando et al. 2016a).

In this paper, we present an updated coincidence search for MeV-scale electron antineutrinos in KamLAND associated with the observed GW events in LIGO-O2 (2016 November 30 to 2017 August 25) and LIGO-O3 (2019 April 1 to March 27).

2. KAMLAND DETECTOR

KamLAND is a large volume liquid scintillator neutrino detector located at the Kamioka mine, 1 km underground from the top of Mt. Ikenoyama in Gifu Prefecture, Japan. The KamLAND detector consists of a cylindrical 10 m radius $\times$ 20 m height water-Cerenkov outer detector for cosmic-ray muon veto, a 9 m radius stainless steel spherical tank that mounts 1325 17-inch and 554 20-inch photomultiplier-tubes (PMTs), and a 6.5 m radius Nylon/EVOH outer balloon filled with approximately 1 kton of ultra-pure liquid scintillator. The liquid scintillator is composed of 20% Pseudocumene (1,2,4-Trimethylbenzene, C_9H_{12}), 80% Dodecane (N-12, $C_{12}H_{26}$), and 1.36 g/l PPO (2,5-Diphenyloxazole, $C_{15}H_{11}NO$). Further details of the KamLAND detector are summarized in Suzuki (2014).

KamLAND began its data acquisition in 2002 March. The detector was upgraded in 2011 August to include a drop-shaped 1.5 m-radius nylon inner balloon filled with approximately 400 kg of purified xenon loaded in liquid scintillator (Gando et al. 2016b). In this configuration, known as the KamLAND-Zen 400 experiment, KamLAND searched for neutrinoless double-beta decay until 2015 December, at which point the inner balloon was removed. Subsequently in 2018 May, a further upgrade to the KamLAND-Zen 800 experiment ensued with the addition of a 1.9 m-radius inner balloon, containing approximately 800 kg of purified xenon.

Electronic boards record the digitized PMT waveforms and provid the corresponding time stamp based on a 40 MHz internal clock. All internal clocks are synchronized to the Unix Time Stamp on every 32nd pulse per second (1 PPS) trigger from a Global Positioning System receiver, located at the entrance to the Kamioka mine. Uncertainties in the absolute trigger time stamp accuracy are less than $\mathcal{O}(100)\,\mu$s, derived from the signal transportation into the mine, optical/electrical signal conversion, and triggering electronics, which is negligibly small for this coincidence search.

The interaction vertex and energy deposition are reconstructed using the measured PMT charge and timing information. At low energies, the detector calibrations are performed using various radioactive sources: ^{60}Co, ^{68}Ge, ^{203}Hg, ^{65}Zn, ^{241}Am^{9}Be, ^{137}Cs, and ^{210}Po^{13}C. At higher energies (>10 MeV), the energy response is calibrated using spallation-produced ^{12}B/^{12}N. Daily stability measurements are performed using the 2.2 MeV gamma ray emitted from a spallation-neutron capture on a proton (Abe et al. 2010). The reconstructed energy and interaction vertex resolution are evaluated as $6.4\%/\sqrt{E\,(\mathrm{MeV})}$ and ~ 12 cm/$\sqrt{E\,(\mathrm{MeV})}$ (Gando et al. 2013), respectively.

The primary radioactive backgrounds found in the liquid scintillator are $(5.0 \pm 0.2) \times 10^{-18}$ g/g ($93 \pm 4\,\mathrm{nBq/m^3}$) of ^{238}U and $(1.8 \pm 0.1) \times 10^{-17}$ g/g ($59 \pm 4\,\mathrm{nBq/m^3}$) of ^{232}Th (Gando et al. 2015).

During the period in which LIGO-O2 and LIGO-O3 were collecting data, the KamLAND detector had an average livetime efficiency of $\epsilon_{\mathrm{live}} = 0.878$. For all but one GW event in LIGO-O2, GW170608, the KamLAND detector was actively taking physics data. Whereas, three GW events in LIGO-O3 (S191213g, S191215w, and S191216ap) overlapped with an unusual detector condition period. Table 1 and Table 2 summarize the GW events used in this analysis during their respective observing runs, along with the KamLAND detector status.

Table 1. The gravitational wave event list for LIGO-O2 (Abbott et al. 2019) and along with the KamLAND detector status. The three events in which KamLAND has already published the results for a coincidence search (Gando et al. 2016a) are not included in this table.

Gravitational wave	Date and time (UTC)	Distance (Mpc)	Source	KamLAND status
GW170104	2017 January 4, 10:11:58.6	990^{+440}_{-430}	BBH	running
GW170608	2017 June 8, 02:01:16.5	320^{+120}_{-110}	BBH	unusual data condition
GW170729	2017 July 29, 18:56:29.3	2840^{+1400}_{-1360}	BBH	running
GW170809	2017 August 9, 08:28:21.8	1030^{+320}_{-390}	BBH	running
GW170814	2017 August 14, 10:30:43.5	600^{+150}_{-220}	BBH	running
GW170817	2017 August 17, 12:41:04.4	40^{+7}_{-15}	BNS	running
GW170818	2017 August 18, 02:24:09.1	1060^{+420}_{-380}	BBH	running
GW170823	2017 August 23, 13:13:58.5	1940^{+970}_{-900}	BBH	running

3. ELECTRON ANTINEUTRINO SELECTION AND BACKGROUND ESTIMATION

In this analysis, we focus on KamLAND events induced by the electron antineutrino inverse beta-decay (IBD) reaction ($\bar{\nu}_e + p \rightarrow e^+ + n$) with 1.8 MeV neutrino energy threshold. The IBD candidate events can be selected by the delayed coincidence (DC) signature: scintillation light from the positron and its annihilation gamma-rays as a prompt signal, and a 2.2 MeV (4.9 MeV) gamma ray from neutron capture on a proton (carbon-12) as a $207.5 \pm 2.8\,\mu$s delayed signal (Abe et al. 2010). The incident neutrino energy (E_ν) is computed from the reconstructed prompt energy (E_{prompt}) with energy and momentum conservation in the reaction as $E_\nu \simeq E_{\mathrm{prompt}} + 0.78\,\mathrm{MeV} + T_n$, where T_n represents the neutron kinetic energy.

The energy range of this analysis is selected to be E_{prompt} between 0.9–100.0 MeV, with a delayed neutron capture on a proton (carbon-12) energy between 1.8–2.6 MeV (4.4–5.6 MeV). Accidental backgrounds are suppressed by imposing a spatial and time correlation between the prompt and delayed signals. In particular, the reconstructed vertex and time difference between the prompt and delayed signals must be within 200 cm and 0.5–1000 μs of each other. All events must be reconstructed in the fiducial volume region 6 m radius from the center, corresponding to a total number of target protons of $N_T = (5.98 \pm 0.13) \times 10^{31}$. Muon and spallation vetoes are applied after the interaction

Table 2. The gravitational wave event list for LIGO-O3 (Abbott et al. 2019) and KamLAND detector status. Data was extracted from GraceDB (LIGO Scientific Collaboration 2020). The retracted events are not shown here.

Gravitational wave	Date and Time (UTC)	KamLAND status
S190408an	2019 April 8, 18:18:02	running
S190412m	2019 April 12, 05:30:44	running
S190421ar	2019 April 21, 21:38:56	running
S190425z	2019 April 25, 08:18:05	running
S190426c	2019 April 26, 15:21:55	running
S190503bf	2019 May 3, 18:54:04	running
S190510g	2019 May 10, 02:59:39	running
S190512at	2019 May 12, 18:07:14	running
S190513bm	2019 May 13, 20:54:28	running
S190517h	2019 May 17, 05:51:01	running
S190519bj	2019 May 19, 15:35:44	running
S190521g	2019 May 21, 03:02:29	running
S190521r	2019 May 21, 07:43:59	running
S190602aq	2019 June 2, 17:59:27	running
S190630ag	2019 June 30, 18:52:05	running
S190701ah	2019 July 1, 20:33:06	running
S190706ai	2019 July 6, 22:26:41	running
S190707q	2019 July 7, 09:33:26	running
S190718y	2019 July 18, 14:35:12	running
S190720a	2019 July 20, 00:08:36	running
S190727h	2019 July 27, 06:03:33	running
S190728q	2019 July 28, 06:45:10	running
S190814bv	2019 August 14, 21:10:39	running
S190828j	2019 August 28, 06:34:05	running
S190828l	2019 August 28, 06:55:09	running
S190901ap	2019 September 1, 23:31:01	running
S190910d	2019 September 10, 01:26:19	running
S190910h	2019 September 10, 08:29:58	running
S190915ak	2019 September 15, 23:57:02	running
S190923y	2019 September 23, 12:55:59	running
S190924h	2019 September 24, 02:18:46	running
S190930s	2019 September 30, 13:35:41	running
S190930t	2019 September 30, 14:34:07	running
S191105e	2019 November 5, 14:35:21	running
S191109d	2019 November 9, 01:07:17	running
S191129u	2019 November 29, 13:40:29	running
S191204r	2019 December 4, 17:15:26	running
S191205ah	2019 December 5, 21:52:08	running
S191213g	2019 December 13, 15:59:05	unusual data condition
S191215w	2019 December 15, 22:30:52	unusual data condition
S191216ap	2019 December 16, 21:33:38	unusual data condition
S191222n	2019 December 22, 03:35:37	running
S200105ae	2020 January 5, 16:24:26	running
S200112r	2020 January 12, 15:58:38	running
S200114f	2020 January 14, 02:08:18	running
S200115j	2020 January 15, 04:23:09	running
S200128d	2020 January 28, 02:20:11	running
S200129m	2020 January 29, 06:54:58	running
S200208q	2020 February 8, 13:01:17	running
S200213t	2020 February 13, 04:10:40	running
S200219ac	2020 February 19, 09:44:15	running
S200224ca	2020 February 24, 22:22:34	running
S200225q	2020 February 25, 06:04:21	running
S200302c	2020 March 2, 01:58:11	running
S200311bg	2020 March 11, 11:58:53	running
S200316bj	2020 March 16, 21:57:56	running

of a cosmic-ray muon, which occur at a rate of approximately 0.34 Hz in KamLAND. Further details regarding the event selection can be found in previous KamLAND analyses (Gando et al. 2011, 2013; Asakura et al. 2015; Gando et al. 2016a). A likelihood-based signal selection distinguishes electron antineutrino DC pairs from accidental coincidence backgrounds for a few to several MeV energy range. This has been updated from the previous analyses considering the accidental coincidence event rates, upgraded detector conditions of the outer detector refurbishment (Ozaki & Shirai 2017), inner balloon installation for KamLAND-Zen 800 (Gando 2020), and the activity of Japanese nuclear reactors.

From 2018 May onwards (the KamLAND-Zen 800 phase) – in order to avoid unexpected background contamination due to the xenon-loaded liquid scintillator, inner balloon body, and suspending ropes – the inner balloon region is vetoed for the delayed event. The inner-balloon cut regions are: a 2.5 m radius spherical volume centered in the detector and a 2.5 m radius vertical cylindrical volume in the upper-half of detector. In this analysis, the effect of this additional inner balloon cut is considered as a selection efficiency suppression for the delayed event rather than a change in the number of target protons for the prompt event. Therefore, the total selection efficiencies are different between the KamLAND datasets corresponding to the periods operating during LIGO-O2 (without the inner balloon cut) and LIGO-O3 (with the additional inner balloon cut).

The selection efficiencies are shown in Figure 1, as a function of the reconstructed prompt energy ($\epsilon_{\rm s}(E_{\rm prompt})$). The structure of the efficiency suppression around $E_{\rm prompt} \simeq 2$ MeV is primarily derived from the accidental background spectrum shape. Above $E_{\rm prompt} = 5.0$ MeV, at which point the accidental background contamination becomes negligibly small, the selection efficiencies in each dataset converge to 92.9% and 77.4%.

The dominant neutrino sources below 8 MeV are the Japanese reactor power plants and geo-chemical radioactive decays in the Earth. After the Great East Japan Earthquake on 2011 March 11, most of the reactors in Japan were shut down and only a few have since been brought back online. Other backgrounds are DC pairs of accidental radioisotopes, spallation products ^{9}Li, and ^{13}C(α, n)^{16}O reaction. Above ∼10 MeV, fast neutrons from cosmic-ray muons and atmospheric neutrino interactions are the dominant contribution to the background (Gando et al. 2012).

4. COINCIDENCE EVENT SEARCH

This analysis is performed using a coincident time window of ±500 s around each of the 60 GW events listed in Table 1 and Table 2. The selected timing window is based on the largest expected time gap between GW events and neutrino events (Baret et al. 2011). This is sufficiently large to cover possible early neutrino emission scenarios as well as the neutrino time-of-flight delay from GW170729, the most distant GW source in this analysis. For example, assuming the sum of neutrino mass limits and cosmological constants from Aghanim et al. (2018), and the neutrino mass-squared splittings from Esteban et al. (2019), a neutrino with an energy of 1.8 MeV, upper mass state of 60 meV, traveling a distance of 2840 Mpc will be delayed by approximately 86 s relative to the GW.

The expected number of uncorrelated background events per ±500 s time window are estimated using off-time windows from the GW and found to be 4.08×10^{-3} and 4.27×10^{-3} for the KamLAND periods corresponding to LIGO-O2 and LIGO-O3, respectively.

No IBD electron antineutrino events were found in the KamLAND dataset within ±500 s of each GW event. Using the uncorrelated accidental background rates and zero observed signal events, the Feldman-Cousins method (Feldman & Cousins 1998) is used to derive the 90% confidence level (C.L.)

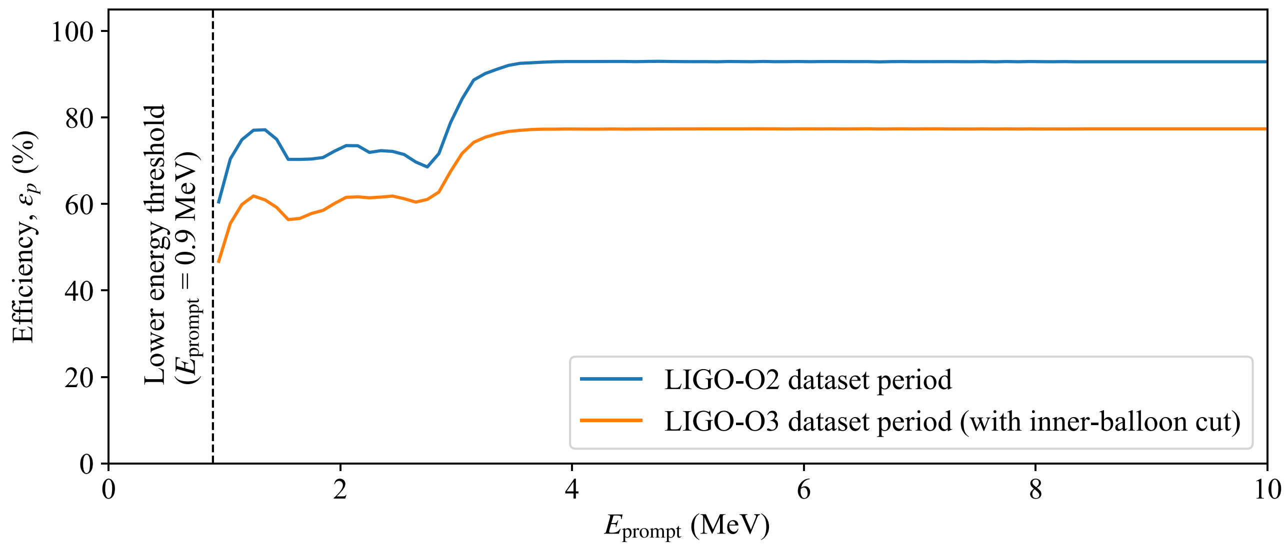

Figure 1. The electron antineutrino selection efficiencies as a function of the prompt energy. The analysis period is divided into two datasets: the LIGO-O2 period in which we use of the full fiducial volume of the KamLAND detector (blue) and the LIGO-O3 period which includes the additional inner balloon cut described in the text. At a few MeV, the selection efficiencies are reduced by the likelihood selection to suppress the contamination of accidental coincidence. The vertical dashed line represents a lower energy threshold of $E_{\text{prompt}} \geqq 0.9\,\text{MeV}$.

upper limit on the number of detected electron antineutrinos. This is found to be $N_{90} = 2.435$ for each GW event in the LIGO-O2 and $N_{90} = 2.435$ for each GW event in the LIGO-O3. The upper limit (F_{90}) can then be used to place constraints on the neutrino fluence, as follows:

$$F_{90} = \frac{N_{90}}{N_T\,\epsilon_{\text{live}} \int \epsilon_{\text{s}}(E_{\text{prompt}}(E'_\nu))\,\sigma(E'_\nu)\,\lambda(E'_\nu)\,dE'_\nu}, \tag{1}$$

where $\sigma(E_\nu)$ is the IBD cross section (Strumia & Vissani 2003) and $\lambda(E_\nu)$ is the neutrino energy spectrum. In order to perform a model independent analysis from the neutrino emission mechanisms for various GW sources, we assume a monochromatic neutrino energy spectra. Hence, we calculate 90% C.L. fluence upper limits on the electron antineutrinos for each GW event in LIGO-O2 and LIGO-O3 with

$$F_{90}(E_\nu) = \frac{N_{90}}{N_T\,\epsilon_{\text{live}}\,\epsilon_{\text{s}}(E_\nu)\,\sigma(E_\nu)}, \tag{2}$$

as shown in Figure 2. The resulting upper limits on the electron antineutrino fluence are found to be between 10^8–$10^{13}\,\text{cm}^{-2}$.

We study the neutrino emission energy scales between two cases of GW sources for officially published and detail-known events during LIGO-O2: the BNS merger (BNS: GW170817), and six BBH mergers (BBHs: GW170104, GW170729, GW170809, GW170814, GW170818, GW170823). Because of the $\pm 500\,\text{s}$ coincidence search timing window for each event, the total number of expected background events are 4.08×10^{-3} for the BNS event and 2.45×10^{-2} for the six BBH candidates. Using the Feldman-Cousins method again with the 90% C.L., for zero events observed, the upper limit

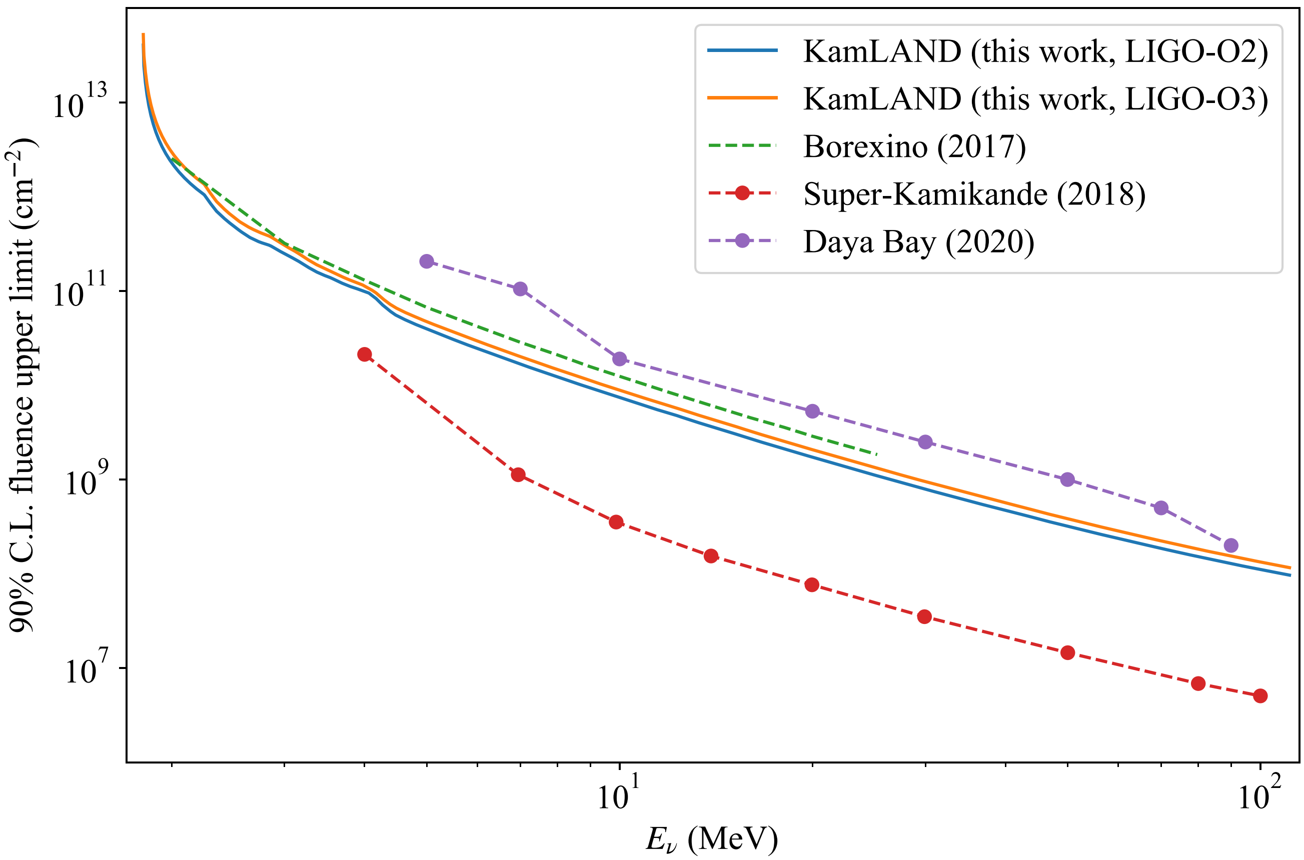

Figure 2. The 90% C.L. electron antineutrino fluence upper limits for each GW. The limits corresponding to events from LIGO-O2 are shown in blue, and events from LIGO-O3 are shown in orange. The difference between the two upper limits are primarily driven by the different selection efficiencies shown in Figure 1. For comparison, the 90% C.L. fluence upper limits on electron antineutrinos are also shown for Super-Kamiokande (Abe et al. 2018): GW170817; Borexino (Agostini et al. 2017): GW150914, GW151226, and GW170104; and Daya Bay (An et al. 2020): average of GW150914, GW151012, GW151226, GW170104, GW170608, GW170814, and GW170817. Borexino result as the un-binned analysis is shown as a green dashed line, Super-Kamiokande and Daya Bay results with binned analysis are shown as red dots and purple dots, respectively.

on the number of neutrino events is $N_{90}^{\rm BNS} = 2.435$ and $N_{90}^{\rm BBHs} = 2.415$ for the BNS and the BBHs respectively. According to Kyutoku & Kashiyama (2018), the assumption that the neutrino energy spectrum has a Fermi-Dirac distribution is reasonable for exploring the mechanism of neutrino emissions from the GW sources. Assuming the Fermi-Dirac distribution, the neutrino energy spectra can be written as

$$\lambda_{\rm FD}(E_\nu) = \frac{1}{T^3 f_2(\eta)} \frac{E_\nu^2}{e^{E_\nu/T-\eta}+1}, \tag{3}$$

$$f_n(\eta) = \int_0^\infty \frac{x^n}{e^{x-\eta}+1} dx, \tag{4}$$

where we assume zero chemical potential and pinching factor $\eta = 0$, the temperature is given as $T = \langle E \rangle / 3.15$, and the average neutrino energy $\langle E \rangle = 12.7\,\mathrm{MeV}$ (Caballero et al. 2016). Integrating between the true electron antineutrino energy limits, $E_\nu = 1.8$–$111\,\mathrm{MeV}$, following Equation (1) and assuming equal contribution from six neutrino species, we obtain upper limits on the total fluence ($\mathcal{F}_{90}^{\mathrm{BNS,\ BBH}}$) in the Fermi-Dirac distribution case with 90% C.L. as

$$\mathcal{F}_{90}^{\mathrm{BNS}} \leq 2.04 \times 10^{10}\,\mathrm{cm}^{-2} \tag{5}$$

for the BNS and

$$\mathcal{F}_{90}^{\mathrm{BBH}} \leq 2.02 \times 10^{10}\,\mathrm{cm}^{-2} \tag{6}$$

for the BBH. Considering the luminosity distances from the GW source, we convert the total fluence ($\mathcal{F}_{90}$) to the total energy ($\mathcal{L}_{90}$) radiated in neutrinos from single source as

$$\mathcal{L}_{90}^{\mathrm{BNS,\ BBH}} = \frac{\mathcal{F}_{90}^{\mathrm{BNS,\ BBH}}}{1/(4\pi D_{\mathrm{eff}}^2 \langle E \rangle)}, \tag{7}$$

where D_{eff} is the effective distance defined as $1/D_{\mathrm{eff}}^2 \equiv \sum_i 1/D_i^2$ for every i-th GW events, and the central values are used to D_i. Hence, the upper limits on the total energy are obtained as

$$\mathcal{L}_{90}^{\mathrm{BNS}} \leq 7.92 \times 10^{58}\,\mathrm{erg} \tag{8}$$

based on the 40 Mpc distance to the BNS event, and

$$\mathcal{L}_{90}^{\mathrm{BBH}} \leq 8.22 \times 10^{60}\,\mathrm{erg} \tag{9}$$

for the BBHs based on the effective distance of 407.6 Mpc, without accounting for neutrino oscillation effects. The observed upper limits are found to be larger than the typical total energy radiated from supernovae $\mathcal{O}(10^{53})$ erg (Bethe 1990).

5. SUMMARY

This paper searched for coincident IBD electron antineutrinos in KamLAND with the 60 GW events associated with the second and third observing runs of the LIGO detector. No coincident signal was observed within a ± 500 s timing window around each GW event. The 90% C.L. electron antineutrino fluence upper limit for each GW, assuming a mono-energetic neutrino flux, was presented for neutrino energies between 1.8 MeV and 111 MeV. We set the most strict upper limit on each GW event in the LIGO-O2 dataset below 3.5 MeV neutrino energies. For the LIGO-O3 dataset, this is the first result of an MeV-scale energy coincidence neutrino search.

The obtained upper limits on the total energy radiated from GW source class, BNS or BBH, in LIGO-O2 with the assumption of a Fermi-Dirac neutrino energy distribution, are found to be 7.92×10^{58} erg and 8.22×10^{60} erg, respectively. These results depend on the number of GW events and distances. This limit will be improved once the candidate events of LIGO-O3 are published.

In the future, the mechanism of neutrino emission may be constrained and explored by combining with multi-messenger astronomy: GeV/TeV neutrino detectors, X-ray/gamma-ray telescopes, and gravitational wave detectors. The KamLAND detector continues to take physics data while running in the KamLAND-Zen 800 configuration and is monitoring for transient astrophysical events. The recently implemented online monitor at KamLAND (Asakura et al. 2016) also readily searches for correlations with transient events and reports the results to the Gamma-ray Coordinates Network (GCN) and/or the Astronomer's Telegram (ATel).

ACKNOWLEDGMENTS

The KamLAND experiment is supported by JSPS KAKENHI Grants 19H05803; the World Premier International Research Center Initiative (WPI Initiative), MEXT, Japan; Netherlands Organisation for Scientific Research (NWO); and under the U.S. Department of Energy (DOE) Contract No. DE-AC02-05CH11231, the National Science Foundation (NSF) No. NSF-1806440, NSF-2012964, as well as other DOE and NSF grants to individual institutions. The Kamioka Mining and Smelting Company has provided service for activities in the mine. We acknowledge the support of NII for SINET4. This work is partly supported by the Graduate Program on Physics for the Universe (GP-PU), and the Frontier Research Institute for Interdisciplinary Sciences, Tohoku University.

REFERENCES

Aartsen, M., Abbasi, R., Abdou, Y., et al. 2013, Science, 342

Aartsen, M. G., Ackermann, M., Adams, J., et al. 2020, The Astrophysical Journal, 898, L10, doi: 10.3847/2041-8213/ab9d24

Abbott, B. P., Abbott, R., Abbott, T. D., et al. 2016, Phys. Rev. Lett., 116, 061102, doi: 10.1103/PhysRevLett.116.061102

Abbott, B. P., Abbott, R., Abbott, T., et al. 2017a, Physical Review Letters, 119, 161101

Abbott, B. P., Abbott, R., Abbott, T. D., et al. 2017b, The Astrophysical Journal, 848, L12, doi: 10.3847/2041-8213/aa91c9

—. 2019, Phys. Rev. X, 9, 031040, doi: 10.1103/PhysRevX.9.031040

Abe, K., Haga, K., Hayato, Y., et al. 2016, The Astrophysical Journal, 830, L11, doi: 10.3847/2041-8205/830/1/l11

Abe, K., Bronner, C., Hayato, Y., et al. 2018, The Astrophysical Journal, 857, L4, doi: 10.3847/2041-8213/aabaca

Abe, S., Enomoto, S., Furuno, K., et al. 2010, Phys. Rev. C, 81, 025807, doi: 10.1103/PhysRevC.81.025807

Acero, M. A., Adamson, P., Aliaga, L., et al. 2020, Phys. Rev. D, 101, 112006, doi: 10.1103/PhysRevD.101.112006

Adrián-Martínez, S., Albert, A., André, M., et al. 2016, Physical Review D, 93, 122010

Aghanim, N., Akrami, Y., Ashdown, M., et al. 2018, arXiv preprint arXiv:1807.06209

Agostini, M., Altenmüller, K., Appel, S., et al. 2017, The Astrophysical Journal, 850, 21, doi: 10.3847/1538-4357/aa9521

Albert, A., André, M., Anghinolfi, M., et al. 2017a, The Astrophysical Journal, 850, L35, doi: 10.3847/2041-8213/aa9aed

Albert, A., André, M., Anghinolfi, M., et al. 2017b, Phys. Rev. D, 96, 022005, doi: 10.1103/PhysRevD.96.022005

An, F. P., Balantekin, A. B., Band, H. R., et al. 2020, Search For Electron-Antineutrinos Associated With Gravitational-Wave Events GW150914, GW151012, GW151226, GW170104, GW170608, GW170814, and GW170817 at Daya Bay. https://arxiv.org/abs/2006.15386

Asakura, K., Gando, A., Gando, Y., et al. 2015, The Astrophysical Journal, 806, 87

—. 2016, The Astrophysical Journal, 818, 91, doi: 10.3847/0004-637x/818/1/91

Avrorin, A. D., Avrorin, A. V., Aynutdinov, V. M., et al. 2018, JETP Letters, 108, 787, doi: 10.1134/S0021364018240025

Baret, B., Bartos, I., Bouhou, B., et al. 2011, Astroparticle Physics, 35, 1 , doi: https://doi.org/10.1016/j.astropartphys.2011.04.001

Bethe, H. A. 1990, Rev. Mod. Phys., 62, 801, doi: 10.1103/RevModPhys.62.801

Caballero, O. L., Zielinski, T., McLaughlin, G. C., & Surman, R. 2016, Phys. Rev. D, 93, 123015, doi: 10.1103/PhysRevD.93.123015

Collaboration, X., Abe, K., Hiraide, K., et al. 2020, Search for event bursts in XMASS-I associated with gravitational-wave events. https://arxiv.org/abs/2007.16046

Esteban, I., Gonzalez-Garcia, M., Hernandez-Cabezudo, A., Maltoni, M., & Schwetz, T. 2019, Journal of High Energy Physics, 2019, 1

Feldman, G. J., & Cousins, R. D. 1998, Phys. Rev. D, 57, 3873, doi: 10.1103/PhysRevD.57.3873

Foucart, F., Haas, R., Duez, M. D., et al. 2016, Physical Review D, 93, 044019

Gando, A., Gando, Y., Ichimura, K., et al. 2011, Nature Geoscience, 4, 647, doi: 10.1038/ngeo1205

—. 2012, The Astrophysical Journal, 745, 193, doi: 10.1088/0004-637x/745/2/193

Gando, A., Gando, Y., Hanakago, H., et al. 2013, Phys. Rev. D, 88, 033001, doi: 10.1103/PhysRevD.88.033001

—. 2015, Phys. Rev. C, 92, 055808, doi: 10.1103/PhysRevC.92.055808

Gando, A., Gando, Y., Hachiya, T., et al. 2016a, The Astrophysical Journal, 829, L34, doi: 10.3847/2041-8205/829/2/l34

—. 2016b, Phys. Rev. Lett., 117, 082503, doi: 10.1103/PhysRevLett.117.082503

Gando, Y. 2020, Journal of Physics: Conference Series, 1468, doi: 10.1088/1742-6596/1468/1/012142

Halzen, F., & Jaczko, G. 1996, Phys. Rev. D, 54, 2779, doi: 10.1103/PhysRevD.54.2779

Kimura, S. S., Murase, K., Mészáros, P., & Kiuchi, K. 2017, The Astrophysical Journal, 848, L4, doi: 10.3847/2041-8213/aa8d14

Kyutoku, K., & Kashiyama, K. 2018, Phys. Rev. D, 97, 103001, doi: 10.1103/PhysRevD.97.103001

LIGO Scientific Collaboration. 2020, GraceDB (Accessed: 2020-07-04). https://gracedb.ligo.org/superevents/public/O3/

Mészáros, P. 2017, Gamma-Ray Bursts as Neutrino Sources (World Scientific), 1–14, doi: 10.1142/9789814759410_0001

Ozaki, H., & Shirai, J. 2017, PoS, ICHEP2016, 1161, doi: 10.22323/1.282.1161

Sahu, S., & D'Olivo, J. C. 2005, Phys. Rev. D, 71, 047303, doi: 10.1103/PhysRevD.71.047303

Strumia, A., & Vissani, F. 2003, Physics Letters B, 564, 42 , doi: https://doi.org/10.1016/S0370-2693(03)00616-6

Suzuki, A. 2014, The European Physical Journal C, 74, doi: 10.1140/epjc/s10052-014-3094-x